

Selective Orientation of Chiral Molecules by Laser Fields with Twisted Polarization

I. Tutunnikov, E. Gershnel, S. Gold, and I. Sh. Averbukh

Department of Chemical and Biological Physics, Weizmann Institute of Science, Rehovot 7610001, ISRAEL

We explore a pure optical method for enantioselective orientation of chiral molecules by means of laser fields with twisted polarization. Several field implementations are considered, including a pair of delayed cross-polarized laser pulses, an optical centrifuge, and polarization shaped pulses. The underlying classical orientation mechanism common for all these fields is discussed, and its operation is demonstrated for a range of chiral molecules of various complexity: hydrogen thioperoxide (HSOH), propylene oxide ($\text{CH}_3\text{CHCH}_2\text{O}$) and ethyl oxirane ($\text{CH}_3\text{CH}_2\text{CHCH}_2\text{O}$). The presented results demonstrate generality, versatility and robustness of this optical method for manipulating molecular enantiomers in the gas phase.

I. INTRODUCTION

Chiral compounds are missing mirror symmetry and cannot be superimposed with their reflection in a flat mirror [1–3]. Chiral molecules related by such a reflection are called enantiomers. An important research direction is chiral resolution; a problem of differentiation of enantiomers in a mixture containing both of them. The ability to separate the enantiomers is a crucial step in drug synthesis, as different enantiomers of chiral drugs exhibit marked distinctions in their biological activity [4]. The related studies focus on the measurements of enantiomeric excess, handedness of a given compound and devising techniques for manipulating mixtures containing both enantiomers [5–16]. Traditional chiral resolution methods include crystallization, chromatography and using enantioselective enzymes. Recently, a number of new techniques have been developed for investigating chiral molecules in the gas phase. This includes photoelectron circular dichroism using intense laser pulses or synchrotron radiation [10, 17, 18], Coulomb explosion imaging [8, 9, 19], microwave three-wave mixing [7, 11, 20, 21], and analysis of the laser-induced phase shifts in the microwave signals emitted by rotating dipoles. The later approach was theoretically suggested in [22], based on quantum mechanical arguments and it relied on exciting unidirectional rotation (UDR) of molecules with the help of a pair of nonresonant, delayed cross-polarized laser pulses. This excitation technique had been suggested in [23, 24], further experimentally demonstrated in [25–27], investigated in detail, both from the quantum and classical perspectives in [28] and generalized to chiral trains of multiple pulses in [29, 30]. In a recent paper [31] we showed that linearly polarized laser fields whose polarization axis twists with time in some plane are able to *orient* generic asymmetric molecules. Moreover, we found that the underlying mechanism is classical in nature. The orientation direction is perpendicular to the plane of the polarization rotation, and it is determined by the sense of rotation. Current femtosecond technology offers several options for generating optical fields with twisted polarization. A pair of delayed cross-polarized laser pulses provides the simplest example of such a field, but there are also more complex fields, such as optical centrifuge

[32–35] or polarization shaped pulses [36, 37].

The electric field of the twisted light plays several roles. First of all, it induces *alignment* of the most polarizable molecular axis (for a review of laser molecular alignment, see Refs. [38–42]). The aligned molecular axis tends to follow the rotation of the polarization vector, but due to inertia it experiences an angular lag with respect to it. The skewed rotating field induces the UDR of the axis according to the mechanism described in [23, 24, 28] for linear and symmetric molecules. Moreover, as was shown in [31], in the case of generic asymmetric molecules, the skewed twisting field also induces a torque along the aligned molecular axis, which tends to *orient* the molecules (and their dipole moments) by rotating them about this axis. Enantiomers of chiral asymmetric molecules are mirror images of each other [1–3] and their physical properties, such as permanent dipole moment and polarizability tensor inherit this symmetry relation. The components of the molecular dipole and off-diagonal elements of the polarizability tensor that are connected by the reflection operation have opposite signs for different enantiomers. As a result, the above mechanical torque along the most polarizable axis has opposite signs for different enantiomers as well [31]. This leads to the counter-rotation of their permanent dipole moments, thus causing the out-of-phase time-dependent dipole signals. Therefore, the resulting emission from the gas bears information on the chiral composition of the mixture [22, 31]. The classical nature of the above orientation mechanism ensures generality and operational robustness of the related prospective techniques for detecting and separating enantiomers of chiral molecules.

In this paper, we explore the prospects of using laser fields with twisted polarization for pure optical enantioselective orientation of chiral molecules. Specifically, the chosen laser sources are: (i) a pair of delayed cross-polarized laser pulses [23–27], (ii) optical centrifuge [32–35] and (iii) polarization shaped femtosecond pulses [36, 37]. We examine them in application to three different chiral molecules: hydrogen thioperoxide (HSOH, previously studied in [22, 31]), propylene oxide ($\text{CH}_3\text{CHCH}_2\text{O}$, the first chiral molecule discovered in the interstellar space [43]) and a more complex ethyl oxirane ($\text{CH}_3\text{CH}_2\text{CHCH}_2\text{O}$) molecule. The structure of the pa-

per is as following. In Sec. II, the studied molecules and their properties are presented, followed by the description of the classical model of laser driven rotational dynamics. In Sec. III, a comprehensive analysis of the laser-induced enantioselective orientation is provided. Finally, Section IV summarizes our results and discusses some potential future developments.

II. THE CLASSICAL MODEL

In this paper, we consider chiral molecules as asymmetric classical rigid rotors with an anisotropic polarizability and a permanent dipole moment, which are subject to the three excitation schemes mentioned above. The molecules are presented in Figure 1.

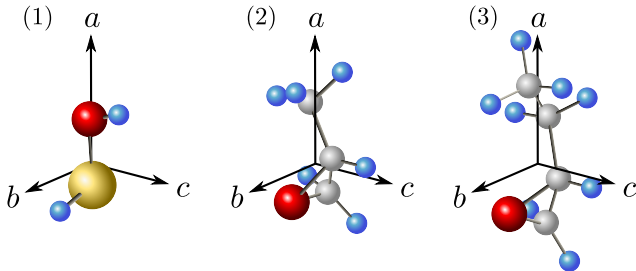


FIG. 1: Molecules under consideration: (1) hydrogen thioperoxide (HSOH), (2) propylene oxide (CH₃CHCH₂O), (3) ethyl oxirane (CH₃CH₂CHCH₂O). Axes a , b and c are the principal axes of the molecules (the moments of inertia are ordered as $I_a < I_b < I_c$). Atoms are color-coded: gray - carbon, blue - hydrogen, red - oxygen, yellow - sulfur.

Table I summarizes the molecular properties. For computation of the molecular electronic properties we used the GAUSSIAN software package (method: CAM-B3LYP/aug-cc-pVTZ) [44].

We investigate the behavior of an ensemble of $N \gg 1$ molecules with the help of the Monte Carlo simulation in which rotational dynamics of each molecule is treated numerically. There is a well known problem with the numerical treatment of rotational dynamics in terms of Euler angles, since it leads to singular equations of motion [45]. Here, we rely on the efficient singularity-free numerical technique, where quaternions are used to parametrize the rotation [46–48]. This solves the problem and also avoids time consuming calculations of trigonometric functions. The orientation of a rigid body is described by a quaternion:

$$q = (q_0, q_1, q_2, q_3) = \left(\cos \frac{\theta}{2}, \sin \frac{\theta}{2} \mathbf{p} \right),$$

where \mathbf{p} is a unit vector defining the direction of rotation and θ is the angle of rotation about it. The rate of change in time of a quaternion is given by

$$\dot{q} = \frac{1}{2} q \Omega, \quad (1)$$

Molecule	Moments of inertia	Polarizability tensor components	Dipole moment components
Hydrogen thioperoxide	$I_a = 16215$	$\alpha_{aa} = 32.04$ $\alpha_{ab} = -1.21$	$\mu_a = 0.020$
	$I_b = 215759$	$\alpha_{bb} = 26.72$ $\alpha_{ac} = 0.65$	$\mu_b = 0.765$
	$I_c = 221933$	$\alpha_{cc} = 26.78$ $\alpha_{bc} = -0.03$	$\mu_c = 1.435$
Propylene oxide	$I_a = 180386$	$\alpha_{aa} = 45.63$ $\alpha_{ab} = 2.56$	$\mu_a = 0.965$
	$I_b = 493185$	$\alpha_{bb} = 37.96$ $\alpha_{ac} = 0.85$	$\mu_b = -1.733$
	$I_c = 553513$	$\alpha_{cc} = 37.87$ $\alpha_{bc} = 0.65$	$\mu_c = 0.489$
Ethyl oxirane	$I_a = 246079$	$\alpha_{aa} = 61.46$ $\alpha_{ab} = 2.17$	$\mu_a = 0.394$
	$I_b = 1001881$	$\alpha_{bb} = 47.97$ $\alpha_{ac} = 1.14$	$\mu_b = -1.878$
	$I_c = 1108231$	$\alpha_{cc} = 47.77$ $\alpha_{bc} = 0.70$	$\mu_c = 0.470$

TABLE I: Summary of molecular properties: eigenvalues of the moment of inertia tensor (atomic units), components of polarizability tensor (atomic units) and components of dipole moment (Debye) in the body-fixed frame of molecular principal axes. For the complimentary enantiomers, the values of α_{ac} , α_{bc} and μ_c have the opposite sign.

where $\Omega = (0, \mathbf{\Omega})$ is a pure quaternion [47, 48] constructed from angular velocity of the molecule, expressed with respect to the body-fixed frame of molecular principal axes a , b and c , $\mathbf{\Omega} = (\Omega_a, \Omega_b, \Omega_c)$. In Eq. 1, quaternions multiplication rule is implied [47, 48]. According to Euler equations [45], the rate of change of the angular velocity expressed with respect to body-fixed frame is

$$\vec{\mathbf{I}} \dot{\Omega} = (\vec{\mathbf{I}} \Omega) \times \Omega + \mathbf{T}, \quad (2)$$

where $\vec{\mathbf{I}}$ is the moment of inertia tensor and $\mathbf{T} = (T_a, T_b, T_c)$ is the torque, both expressed with respect to the body-fixed frame. To model the torque due to interaction with an electric field, we transform the electric field \mathcal{E} , expressed with respect to the laboratory frame of reference, into the body-fixed frame. The transformation law is $E = q^c \mathcal{E} q$, where $E = (0, \mathbf{E})$ and $\mathcal{E} = (0, \mathbf{\mathcal{E}})$ are pure quaternions, constructed from the electric field in the body-fixed frame and \mathcal{E} , respectively. A conjugate of a quaternion q is denoted by q^c [47, 48]. Again, quaternions multiplication rule is used in the transformation. The induced dipole moment in the body-fixed principal axes frame is given by $\mathbf{D} = \vec{\alpha} \mathbf{E}$, where $\vec{\alpha}$ is the polarizability tensor in the body-fixed frame. Then, the torque is $\mathbf{T} = \mathbf{D} \times \mathbf{E}$. We integrate the system of Eqs. 1 and 2 using the Runge-Kutta integration method. We renormalize the quaternions at each time step in order to preserve the unit norm [46, 48].

In our simulations, the initial conditions for the ensemble of molecules are set up via a Monte Carlo procedure. The initial orientations of the molecules and the corresponding quaternions for an isotropic ensemble are generated by a random uniform sampling over the space of rotations [49]. We assume that the molecular ensemble

is initially at thermal conditions, and that the molecular angular velocities are distributed according to:

$$f(\Omega) \propto \exp\left[-\frac{\Omega^T \mathbf{I} \Omega}{2k_B T}\right] = \prod_i \exp\left[-\frac{I_i \Omega_i^2}{2k_B T}\right], \quad (3)$$

where $i = a, b, c$. Since the kinetic energy is a scalar, it is coordinate invariant so we express it with respect to the body-fixed frame. Here, T is the temperature of the gas and k_B is the Boltzmann constant.

III. RESULTS AND DISCUSSION

Following the classical approach presented in Sec. II, we calculated the average Z -projection of the permanent dipole moment, $\langle \mu_Z \rangle(t)$ as a function of time, where Z is the laboratory axis perpendicular to the XY -plane of the polarization twisting, and the angle brackets denote averaging over the ensemble. All the simulations were done for samples of $N = 500,000$ molecules, both at zero temperature and at thermal conditions.

We considered the double pulse excitation scheme [23–27] in application to the rotational dynamics of all three molecules. More sophisticated schemes, involving optical centrifuge [32–35] and polarization shaped pulses [36] were examined in application to propylene oxide and ethyl oxirane molecules.

A. Enantioselective orientation by double pulse excitation scheme

In this excitation scheme, the molecules are subject to a pair of delayed cross-polarized laser pulses. The pulses are Gaussian-shaped in time. The peak intensity of the pulses is $I_0 = 17.7 \times 10^{12} \text{ W/cm}^2$, their duration (FWHM) is 0.1 ps, which is short compared with the typical periods of the molecular rotation. Both pulses propagate along the Z axis. The first pulse has its maximum at $t = 0$, and is polarized along the X direction, while the polarization vector of the second pulse is in the XY plane, at 45° to the X direction. The first pulse induces alignment of the most polarizable axis of the molecule along the X direction [38–42]. Figure 2 shows the time dependent alignment factor, $\langle \cos^2(\theta_X) \rangle(t)$ for hydrogen thioperoxide molecules. Here, θ_X is the angle between the most polarizable a -axis of the molecules and the polarization direction of the first pulse (X axis). At zero initial temperature (Fig. 2a), the alignment factor demonstrates decaying oscillations with several local maxima. The first (most intense) peak appears at $t = 0.32$ ps. At $T = 50\text{K}$ (Fig. 2b) a pronounced single alignment maximum appears shortly after the first pulse, at $t = 0.27$ ps. The oscillations decay rapidly due to the thermal dispersion of rotational velocities. Notice that a permanent alignment above the isotropic value of $1/3$ is seen in the long-term run.

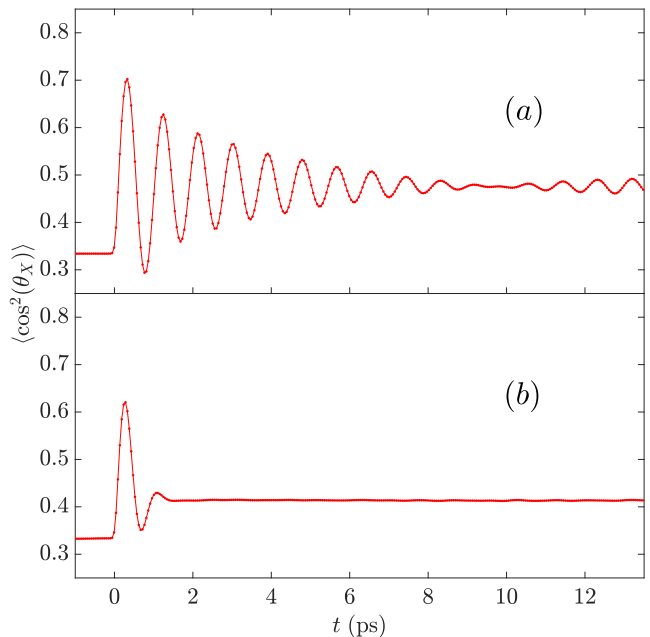


FIG. 2: Alignment factor as a function of time, $\langle \cos^2(\theta_X) \rangle(t)$ for hydrogen thioperoxide molecules. (a) $T = 0\text{K}$, first alignment maximum at $t = 0.32$ ps; (b) $T = 50\text{K}$, first alignment maximum at $t = 0.27$ ps.

The second laser pulse applied to the aligned molecules induces UDR of the most polarizable molecular axis about the Z direction. The sense of this unidirectional motion is the same for both enantiomers. However, since the studied molecules are asymmetric, this pulse also initiates a rotation about the aligned molecular axis [31]. The later rotation leads to the enantioselective orientation of the permanent dipole moments perpendicular to the plane of the pulses, along Z axis [22, 31]. Those effects are most emphasized when the second pulse is applied at the instance of a well developed alignment. In our simulations, we chose the delay of the second pulse at the moment of the most intense peak of the alignment factor, $\langle \cos^2(\theta_X) \rangle(t)$.

Figure 3a shows the ensemble-averaged dipole moment, $\langle \mu_Z \rangle(t)$ for two enantiomers of hydrogen thioperoxide molecule, subject to the double pulse excitation. As seen in the figure, $\langle \mu_Z \rangle$ is zero just after the first pulse, which is consistent with the symmetry of the pulse interaction with the induced molecular polarization. However, a pronounced dipole signal emerges shortly after the application of the second pulse. Moreover, one can observe an out-of-phase evolution of the dipole signals produced by different enantiomers. The reason for such a behavior stems from the mirror symmetry of the enantiomers, namely by the fact that the components of the molecular dipole and off-diagonal elements of the polarizability tensor, which are connected by reflection have opposite signs for different enantiomers [22, 31].

Figure 3b shows $\langle \mu_Z \rangle(t)$ for hydrogen thioperoxide molecules at $T = 50\text{K}$. Here, the magnitude of the dipole

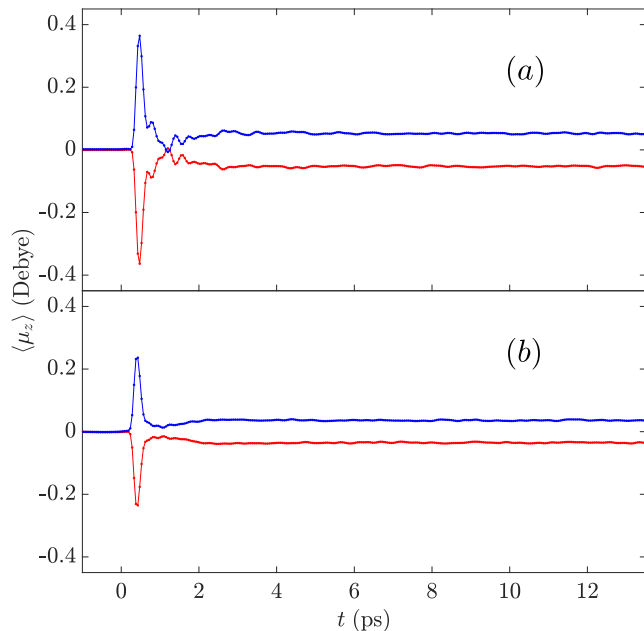


FIG. 3: Average Z-projection of the dipole moment of both enantiomers (blue/red) of hydrogen thioperoxide molecules as a function of time. Excitation: double pulse scheme. (a) $T = 0K$ (the delay of the second pulse is $t = 0.32$ ps). (b) $T = 50K$ (the delay of the second pulse is $t = 0.27$ ps).

signals is lower and fine features of the curve are washed out due to the initial dispersion of angular velocities. Figure 3 shows that the most intense dipole signals appear shortly after the second pulse. However, one can observe a permanent orientation of the dipole moment long after the end of the second pulse. The average value of this permanent orientation is comparable to the peak values achieved just after the second pulse. Long-term permanent orientation at field-free conditions does not exist for linear polar molecules, since the individual dipoles of the molecules are always perpendicular to the conserved vectors of angular momentum, and they perform planar rotation with dispersed angular velocities. In the case of asymmetric molecules considered here, they perform a precession-like free motion. As a result, a non-zero time averaged projection of the dipole moment along the oriented angular momentum exists, leading to the observed permanent orientation.

Figure 2b shows that even a single laser pulse creates a permanent field-free alignment (not orientation) in the molecular ensemble. This permanent alignment may serve as a resource for orienting molecules with the help of the second laser pulse via the same mechanism as described above. Clearly, in this regime the exact timing of the second pulse is not important, as illustrated in Figure 4. Notice that here the permanent dipole moment is reduced compared to Figure 3, since the delay of the second pulse in all three shown cases is far from the optimal ($t = 0.27$ ps).

We performed a similar analysis for the two additional

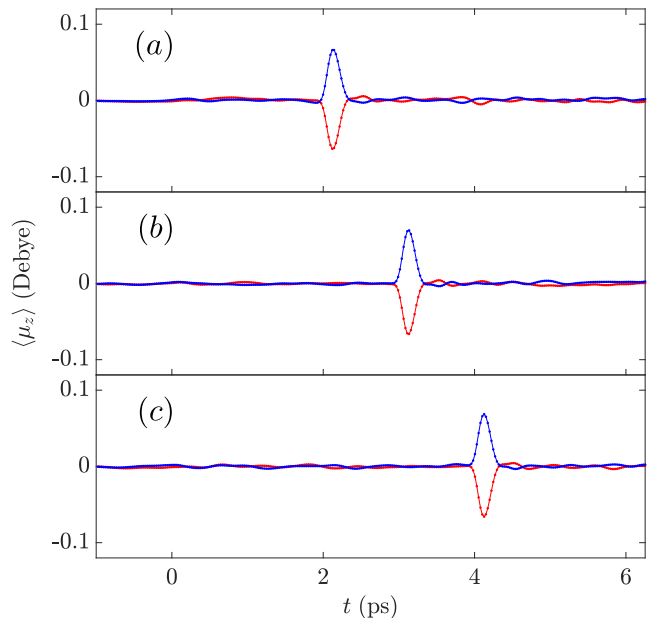


FIG. 4: Average Z-projection of the dipole moment of both enantiomers (blue/red) of hydrogen thioperoxide molecules as a function of time, $T = 50K$. Excitation: double pulse scheme. Delay of the second pulse is: (a) $t = 2$ ps, (b) $t = 3$ ps, (c) $t = 4$ ps.

molecules - propylene oxide and ethyl oxirane excited by a pair of cross-polarized pulses. Table II shows the times of the first maximum of the alignment factor for all three molecules considered in this paper. Figure 5 shows $\langle \mu_z \rangle(t)$ for both enantiomers of the propylene oxide molecules at $T = 0K$ and $T = 50K$. Similar results for ethyl oxirane molecules are presented in Figure 6. The qualitative behavior of the graphs is similar to that observed in the case of hydrogen thioperoxide molecules, although the characteristic timescales are longer, because of the higher moments of inertia.

Molecule	$T = 0K$	$T = 50K$
Hydrogen thioperoxide	0.32	0.27
Propylene oxide	0.45	0.38
Ethyl oxirane	0.60	0.50

TABLE II: Times of first maximum in the alignment factors for the three considered molecules. Time is measured in picoseconds and counted from the moment of the first pulse.

B. Enantioselective orientation by optical centrifuge

Optical centrifuge (OC) is an optical field in which the polarization vector rotates in plane with an acceleration, β [32–35]. Here, the field propagates along Z direction

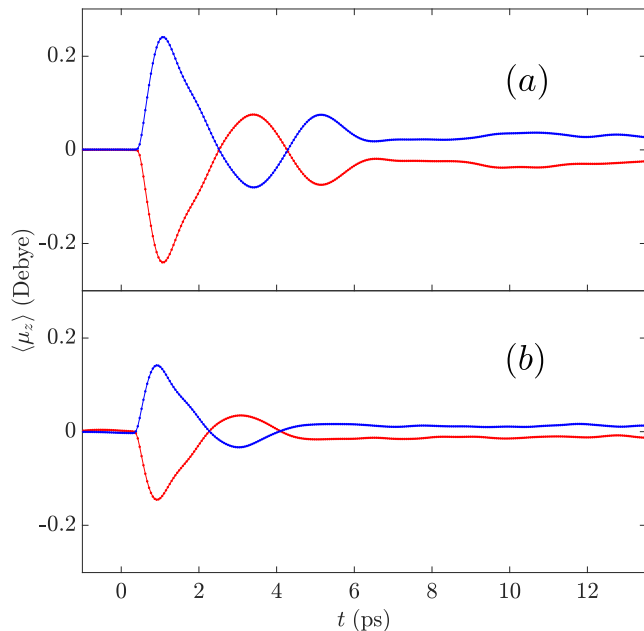


FIG. 5: Average Z -projection of the dipole moment of both enantiomers (blue/red) of propylene oxide molecules as a function of time. Excitation: double pulse scheme. (a) $T = 0K$ (the delay of the second pulse is $t = 0.45$ ps). (b) $T = 50K$ (the delay of the second pulse is $t = 0.38$ ps).

while its polarization vector rotates in the XY plane. The most polarizable molecular axis is expected to follow the accelerated rotation of the field in the XY plane. The molecules may also execute some small amplitude out-of-plane oscillations while following the field. The question whether a particular molecule is indeed following the polarization vector of the field, or in other words is “captured” by the centrifuge, is not a trivial one. The answer depends on the parameters of the OC, and the initial conditions of the molecules - angular velocity of the molecule and its initial orientation with respect to the polarization. In the special cases of linear and symmetric molecules, the OC operation was studied numerically in [50, 51]. Recently, an analytical study of the OC using the theory of classical autoresonance [52], as well as its quantum mechanical counterpart [53] was done. A detailed theory for optical centrifugation of asymmetric molecules is yet to be developed. However, it is clear at the qualitative level, that if a molecule is indeed captured in the regime of steady angular acceleration, its most polarizable axis follows the rotating polarization vector with some angular lag depending on the acceleration value. This is quite similar to the deviation of the suspended pendulum from the vertical position when the suspension point moves with horizontal acceleration. Thus, the situation is analogous to that of a double pulse excitation scheme described in Subsection III A. The field of the optical centrifuge aligns the most polarizable axis of the accelerating molecules close to the direction of the rotating polarization. Because of the angular lag, the

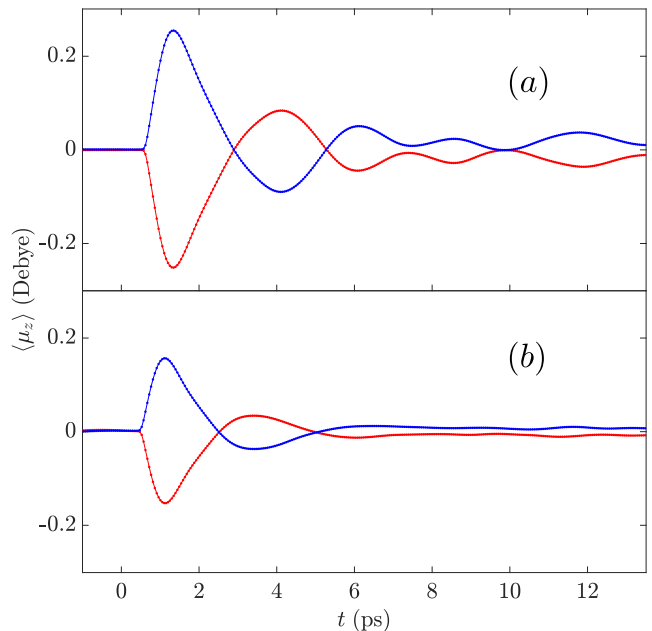


FIG. 6: Average Z -projection of the dipole moment of both enantiomers of ethyl oxirane molecules as a function of time. Excitation: double pulse scheme. (a) $T = 0K$ (the delay of the second pulse is $t = 0.60$ ps). (b) $T = 50K$ (the delay of the second pulse is $t = 0.50$ ps).

same field also induces a torque about this direction via the mechanism described in the previous Subsection and in [31]. This makes optical centrifugation promising for enantioselective orientation. Below, we test the feasibility of such an approach, modeling the OC with parameters of the modern experimental setups [34, 35]. We represent the electric field of the optical centrifuge as

$$\mathcal{E} = a(t) [\cos(2\beta t^2) \mathbf{e}_X + \sin(2\beta t^2) \mathbf{e}_Y] \cos(\omega t). \quad (4)$$

Vectors \mathbf{e}_X and \mathbf{e}_Y are the basis unit vectors in the X and Y directions, respectively, $\beta = 0.080 \text{ ps}^{-2}$ is the angular acceleration, ω is the carrier frequency of the light. $a(t)$ is the time dependent field amplitude:

$$a(t) = \mathcal{E}_0 \exp\left(-\frac{t^2}{2\sigma^2}\right) \Theta(\tau - t), \quad (5)$$

where $\mathcal{E}_0 = 0.27 \times 10^{10} \text{ V/m}$ is the peak amplitude of the field, $\sigma = 72 \text{ ps}$, Θ is a unit step function, $\tau = 50 \text{ ps}$ is the cutoff time. Figure 7 shows the amplitude of the electric field, $a(t)$.

The chosen parameters and the shape of the amplitude function of the optical centrifuge are close to those used in recent experiments [54].

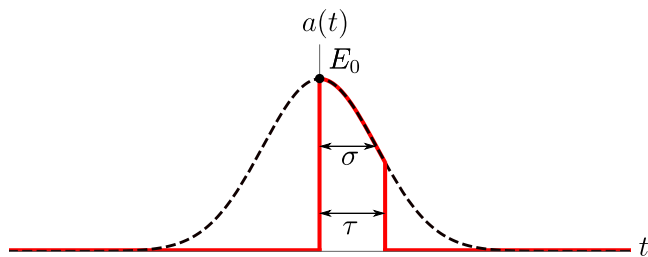


FIG. 7: In red - amplitude, $a(t)$ of electric field of the centrifuge, see equation 5. Dashed black - Gaussian shaped envelope.

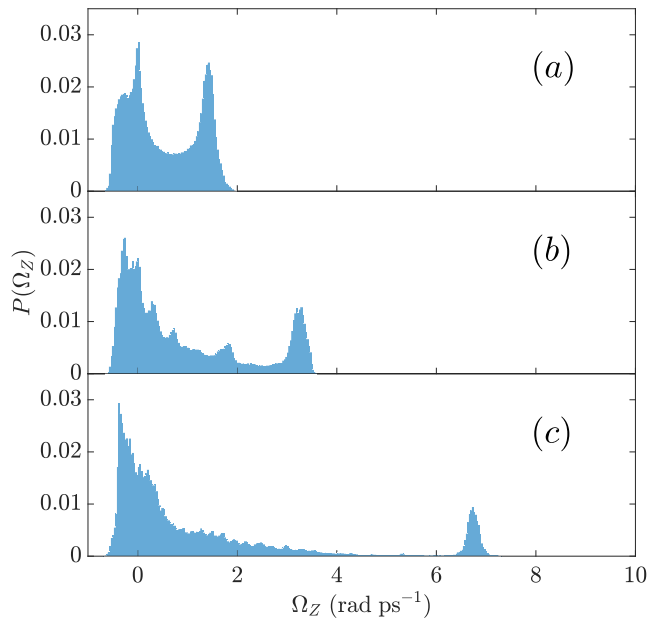


FIG. 8: Projection of angular velocity of propylene oxide molecules on laboratory Z axis, Ω_Z , at consecutive times: (a) $t = 4.5$ ps, (b) $t = 10$ ps, (c) $t = 20$ ps. $T = 0K$. The detached lobe corresponds to the captured molecules and constitutes about 9% of all the molecules (c).

To estimate the fraction of captured molecules, we consider distribution of the projection of angular velocity, Ω_Z on the laboratory Z axis. Figure 8 shows the distribution of Ω_Z for propylene oxide molecules at consecutive times. The initial sharp distribution spreads around zero as a result of the gradually accelerating rotation of the electric field. As the centrifuge speeds up, molecules throughout the distribution attempt to follow the polarization vector and the distribution spreads even more towards the higher values of Ω_Z . Figure 9a shows a pronounced peak in the $\langle \mu_Z \rangle(t)$ graph of propylene oxide shortly after the initiation of the centrifuge. By the time of the peak, the distribution of Ω_Z develops two separated lobes (see Fig. 8a). With time, the lobe advances toward the higher values of Ω_Z and separates completely. The lobe describes the molecules captured by the centrifuge. In Figure 8c, the separated lobe constitutes about 9% of all the molecules, a value typical for

the OC experiments [35].

The average Z -projection of the permanent dipole moment, $\langle \mu_Z \rangle(t)$ for the two enantiomers of propylene oxide are shown in Figure 9a. We can observe a substantial orientation of the permanent dipole moment in the course of the centrifuge operation. Moreover, there is a long-lasting permanent orientation at field-free conditions after the centrifuge cutoff time $\tau = 50$ ps.

Figure 9b shows the average Z -projection of the permanent dipole moment, $\langle \mu_Z \rangle$ for the two enantiomers of ethyl oxirane molecules. Since ethyl oxirane is heavier and has higher moments of inertia than propylene oxide, we chose a smaller value of angular acceleration, $\beta = 0.040$ ps $^{-2}$. The results shown in Figure 9b are qualitatively similar to those presented for propylene oxide molecule in Figure 9a.

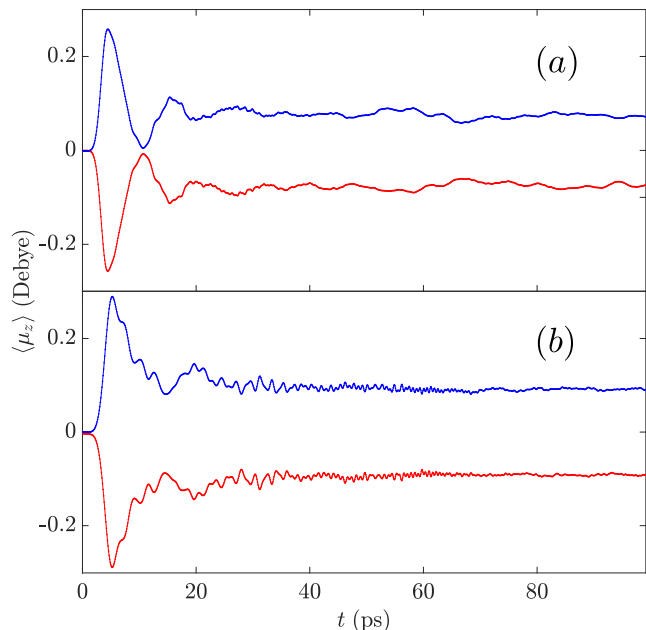


FIG. 9: Average Z -projection of the dipole moment of both enantiomers (blue/red) of (a) propylene oxide and (b) ethyl oxirane molecules as a function of time. Excitation: optical centrifuge. $T = 0K$. The distribution of Ω_Z corresponding to the time of the peak in (a) ($t = 4.5$ ps) is shown in Figure 8a.

C. Enantioselective orientation by polarization shaped laser pulse

In the excitation method using polarizations-shaped pulses with continuously twisted polarization [36], molecules are subject to two short orthogonally polarized and partially overlapped laser pulses. The combination of the pulses creates a field that is continuously twisted. Here, the field propagates along Z direction while its polarization vector twists in the XY plane. Initially, the polarization vector points along the X axis, and then rotates towards the Y direction (see Fig. 10). We model

such a field as

$$\mathcal{E} = [\mathcal{E}_0(t) \cos(\omega t) \mathbf{e}_X + \mathcal{E}_0(t - \tau_p) \cos(\omega t + \varphi_p) \mathbf{e}_Y]. \quad (6)$$

Maximum value of the Gaussian-shaped amplitude, $\mathcal{E}_0(t)$ is $\mathcal{E}_0(0) = 2 \times 10^8$ V/cm, and its duration (FWHM) is 0.141 ps. The delay between the pulses is $\tau_p = 0.150$ ps, ω is the carrier frequency of the light. The relative phase between the two pulses defines the sense of twisting. For φ_p equal to an integer multiple of 2π , the polarization twists in the clockwise direction, while for φ_p equal to an odd multiple of π , it twists in the counterclockwise direction.

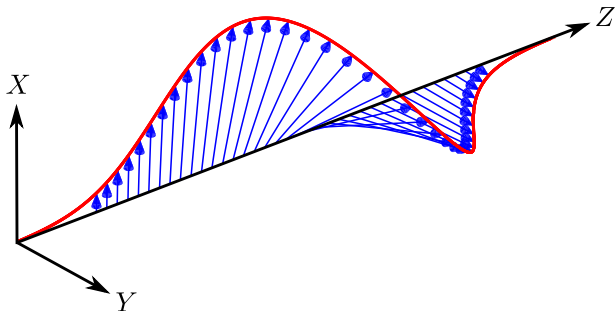


FIG. 10: Illustration of polarization shaped pulse [36, 37]. Here the field twists in the clockwise direction ($\varphi_p = 0$), see equation 6.

Figure 11a shows the time dependent average Z -projection of the permanent dipole moment, $\langle \mu_Z \rangle(t)$, for the two enantiomers of propylene oxide molecules. Figure 11b shows similar results for ethyl oxirane molecules. These dipole signals qualitatively resemble the ones already seen for two other excitation methods.

IV. CONCLUSIONS

It is well known that non-resonant, linearly polarized laser pulses may align molecules along the polarization direction, but cannot orient them because of the symmetry of light interaction with the induced molecular polarization.

In this paper we investigated the mechanism of orientation of generic asymmetric molecules with laser field whose polarization twists with time in some plane. The twisting can be either discrete in time, like in a sequence of delayed cross-polarized laser pulses or continuous, like in optical centrifuge or polarization shaped pulses. In all the cases the rotating polarization induces molecular alignment along a direction close to the polarization vector, and initiates unidirectional rotation of the aligned molecular axis. Importantly, there is an angular lag between the rotating polarization and the aligned molecules because of their inertia. As it was shown in [31], the skewed field also induces rotation about the aligned molecular axis and causes a partial orientation of the molecules and their permanent dipole moments

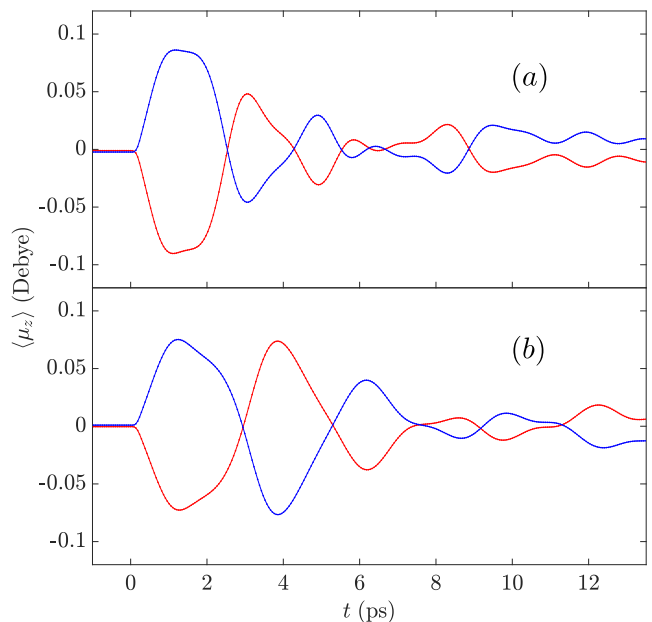


FIG. 11: Average Z -projection of the dipole moment of both enantiomers (blue/red) of (a) propylene oxide and (b) ethyl oxirane molecules as a function of time. Excitation: polarization shaped pulse. $T = 0K$.

along the direction perpendicular to the plane of polarization rotation. It worth mentioning that orientation of the molecular dipoles happens here without any direct interaction between the field and the dipoles, but it results from the controlled rotation of the molecules to which the dipoles are attached. Moreover, this orientation is enantioselective [22, 31] and may be utilized for differentiation of enantiomers. Our results demonstrate generality and robustness of the enantioselective orientation mechanism utilizing various implementation of the laser field with twisted polarization. We examined several specific examples of chiral molecules, including hydrogen thioperoxide, propylene oxide and ethyl oxirane. This selective orientation can be detected in a number of ways, ranging from direct visualization with the help of Coulomb explosion [8, 9, 19] to observation of the out-of-phase oscillations of the enantiomers' dipole moments [22, 31]. In the latter case, the chiral analysis is based on the measurement of laser-induced terahertz emission from the irradiated gas samples [7, 11]. In addition to the significant time-dependent dipole signals from the excited molecules, we predict a substantial field-free permanent dipole orientation persisting long after the laser field is over. This effect can be also used for enantioselective measurements. The described orientation mechanism can be optimized by tuning laser parameters, including the shape of the laser pulses. Consideration of other types of polarization twisting may be useful, including e.g. chiral pulse trains [30] and "laser pulse enantiomers" [55] (also see the references therein). The efficiency of the methods considered here may be improved by combining polarization twist-

ing with other methods of molecular alignment control [38–42, 56, 57]. Deflecting optically pre-oriented chiral molecules by inhomogeneous fields may open new ways for enantiomer separation problem.

V. ACKNOWLEDGEMENTS

Support by the Israel Science Foundation (Grant No. 746/15) is highly appreciated. I.A. thanks V. Milner and

T. Momose for valuable discussions and their hospitality during his stay at the University of British Columbia, Vancouver. We also appreciate helpful discussions with A. Kaplan. The authors gratefully acknowledge M. Iron and P. Oulevey for helping with the quantum-chemical calculations. I.A. acknowledges support as the Patricia Elman Bildner Professorial Chair. This research was made possible in part by the historic generosity of the Harold Perlman Family.

-
- [1] G. H. Wagnière. *On Chirality and the Universal Asymmetry: Reflections on Image and Mirror Image*. Wiley-VCH, 2007.
- [2] F. A. Cotton. *Chemical Applications of Group Theory*. John Wiley & Sons: New York, 1990.
- [3] J. P. Riehl. *Mirror-Image Asymmetry: An Introduction to the Origin and Consequences of Chirality*. Wiley, 2010.
- [4] L. A. Nguyen, H. He, and C. Pham-Huy. Chiral drugs: An overview. *International Journal of Biomedical Science: IJBS*, 2(2):85–100, Jun 2006.
- [5] Y. Li and C. Bruder. Dynamic method to distinguish between left- and right-handed chiral molecules. *Phys. Rev. A*, 77:015403, Jan 2008.
- [6] Y. He, B. Wang, R. K. Dukor, and L. A. Nafie. Determination of absolute configuration of chiral molecules using vibrational optical activity: A review. *Applied Spectroscopy*, 65(7):699–723, 2011. PMID: 21740631.
- [7] D. Patterson, M. Schnell, and J. M. Doyle. Enantiomer-specific detection of chiral molecules via microwave spectroscopy. *Nature*, 497(7450):475–477, May 2013.
- [8] M. Pitzer, M. Kunitski, A. S. Johnson, T. Jahnke, H. Sann, F. Sturm, L. Ph. H. Schmidt, H. Schmidt-Böcking, R. Dörner, J. Stöhner, J. Kiedrowski, M. Reggelin, S. Marquardt, A. Schießler, R. Berger, and M. S. Schöffler. Direct determination of absolute molecular stereochemistry in gas phase by Coulomb explosion imaging. *Science*, 341(6150):1096–1100, 2013.
- [9] P. Herwig, K. Zawatzky, M. Grieser, O. Heber, B. Jordon-Thaden, C. Krantz, O. Novotný, R. Repnow, V. Schurig, D. Schwalm, Z. Vager, A. Wolf, O. Trapp, and H. Kreckel. Imaging the absolute configuration of a chiral epoxide in the gas phase. *Science*, 342(6162):1084–1086, 2013.
- [10] M. H. M. Janssen and I. Powis. Detecting chirality in molecules by imaging photoelectron circular dichroism. *Phys. Chem. Chem. Phys.*, 16:856–871, 2014.
- [11] D. Patterson and M. Schnell. New studies on molecular chirality in the gas phase: enantiomer differentiation and determination of enantiomeric excess. *Phys. Chem. Chem. Phys.*, 16:11114–11123, 2014.
- [12] K. Bodenhofer, A. Hierlemann, J. Seemann, G. Gauglitz, B. Koppenhoefer, and W. Gpel. Chiral discrimination using piezoelectric and optical gas sensors. *Nature*, 387(6633):577–580, Jun 1997.
- [13] R. McKendry, M.-E. Theoclitou, T. Rayment, and C. Abell. Chiral discrimination by chemical force microscopy. *Nature*, 391(6667):566–568, Feb 1998.
- [14] G. L. J. A. Rikken and E. Raupach. Enantioselective magnetochiral photochemistry. *Nature*, 405(6789):932–935, Jun 2000.
- [15] H. Zepik, E. Shavit, M. Tang, T. R. Jensen, K. Kjaer, G. Bolbach, L. Leiserowitz, I. Weissbuch, and M. Lahav. Chiral amplification of oligopeptides in two-dimensional crystalline self-assemblies on water. *Science*, 295(5558):1266–1269, 2002.
- [16] P. Král, I. Thanopoulos, M. Shapiro, and D. Cohen. Two-step enantio-selective optical switch. *Phys. Rev. Lett.*, 90:033001, Jan 2003.
- [17] N. Böwering, T. Lischke, B. Schmidtke, N. Müller, T. Khalil, and U. Heinzmann. Asymmetry in photoelectron emission from chiral molecules induced by circularly polarized light. *Phys. Rev. Lett.*, 86:1187–1190, Feb 2001.
- [18] C. Lux, A. Senftleben, C. Sarpe, M. Wollenhaupt, and T. Baumert. Photoelectron circular dichroism observed in the above-threshold ionization signal from chiral molecules with femtosecond laser pulses. *Journal of Physics B: Atomic, Molecular and Optical Physics*, 49(2):02LT01, 2016.
- [19] M. Pitzer. How to determine the handedness of single molecules using Coulomb explosion imaging. *Journal of Physics B: Atomic, Molecular and Optical Physics*, 50(15):153001, 2017.
- [20] D. Patterson and J. M. Doyle. Sensitive chiral analysis via microwave three-wave mixing. *Phys. Rev. Lett.*, 111:023008, Jul 2013.
- [21] V. A. Shubert, D. Schmitz, and M. Schnell. Enantiomer-sensitive spectroscopy and mixture analysis of chiral molecules containing two stereogenic centers - microwave three-wave mixing of menthone. *Journal of Molecular Spectroscopy*, 300(Supplement C):31 – 36, 2014. Spectroscopic Tests of Fundamental Physics.
- [22] A. Yachmenev and S. N. Yurchenko. Detecting chirality in molecules by linearly polarized laser fields. *Phys. Rev. Lett.*, 117:033001, Jul 2016.
- [23] S. Fleischer, Y. Khodorkovsky, Y. Prior, and I. Sh. Averbukh. Controlling the sense of molecular rotation. *New Journal of Physics*, 11(10):105039, 2009.
- [24] K. Kitano, H. Hasegawa, and Y. Ohshima. Ultrafast angular momentum orientation by linearly polarized laser fields. *Phys. Rev. Lett.*, 103:223002, Nov 2009.
- [25] O. Korech, U. Steinitz, R. J. Gordon, I. Sh. Averbukh, and Y. Prior. Observing molecular spinning via the rotational Doppler effect. *Nat Photon*, 7(9):711–714, Sep 2013.
- [26] K. Mizuse, K. Kitano, H. Hasegawa, and Y. Ohshima. Quantum unidirectional rotation directly imaged with

- molecules. *Science Advances*, 1(6), 2015.
- [27] K. Lin, Q. Song, X. Gong, Q. Ji, H. Pan, J. Ding, H. Zeng, and J. Wu. Visualizing molecular unidirectional rotation. *Phys. Rev. A*, 92:013410, Jul 2015.
- [28] Y. Khodorkovsky, K. Kitano, H. Hasegawa, Y. Ohshima, and I. Sh. Averbukh. Controlling the sense of molecular rotation: Classical versus quantum analysis. *Phys. Rev. A*, 83:023423, Feb 2011.
- [29] C. Bloomquist, S. Zhdanovich, A. A. Milner, and V. Milner. Directional spinning of molecules with sequences of femtosecond pulses. *Phys. Rev. A*, 86:063413, Dec 2012.
- [30] S. Zhdanovich, A. A. Milner, C. Bloomquist, J. Floß, I. Sh. Averbukh, J. W. Hepburn, and V. Milner. Control of molecular rotation with a chiral train of ultrashort pulses. *Phys. Rev. Lett.*, 107:243004, Dec 2011.
- [31] E. Gershnel and I. Sh. Averbukh. Orienting asymmetric molecules by laser fields with skewed polarization. arXiv:1708.04010 [physics.chem-ph]. 2017.
- [32] J. Karczmarek, J. Wright, P. Corkum, and M. Ivanov. Optical centrifuge for molecules. *Phys. Rev. Lett.*, 82:3420–3423, Apr 1999.
- [33] D. M. Villeneuve, S. A. Aseyev, P. Dietrich, M. Spanner, M. Yu. Ivanov, and P. B. Corkum. Forced molecular rotation in an optical centrifuge. *Phys. Rev. Lett.*, 85:542–545, Jul 2000.
- [34] L. Yuan, S. W. Teitelbaum, A. Robinson, and A. S. Mullin. Dynamics of molecules in extreme rotational states. *Proceedings of the National Academy of Sciences*, 108(17):6872–6877, 2011.
- [35] A. Korobenko, A. A. Milner, and V. Milner. Direct observation, study, and control of molecular superrotors. *Phys. Rev. Lett.*, 112:113004, Mar 2014.
- [36] G. Karras, M. Ndong, E. Hertz, D. Sugny, F. Billard, B. Lavorel, and O. Faucher. Polarization shaping for unidirectional rotational motion of molecules. *Phys. Rev. Lett.*, 114:103001, Mar 2015.
- [37] E. Prost, H. Zhang, E. Hertz, F. Billard, B. Lavorel, P. Bejot, J. Zyss, I. Sh. Averbukh, and O. Faucher. Third-order-harmonic generation in coherently spinning molecules. *Phys. Rev. A*, 96:043418, Oct 2017.
- [38] H. Stapelfeldt and T. Seideman. Colloquium. *Rev. Mod. Phys.*, 75:543–557, Apr 2003.
- [39] Y. Ohshima and H. Hasegawa. Coherent rotational excitation by intense nonresonant laser fields. *International Reviews in Physical Chemistry*, 29(4):619–663, 2010.
- [40] D. Townsend, B. J. Sussman, and A. Stolow. A Stark future for quantum control. *The Journal of Physical Chemistry A*, 115(4):357–373, 2011. PMID: 21182319.
- [41] S. Fleischer, Y. Khodorkovsky, E. Gershnel, Y. Prior, and I. Sh. Averbukh. Molecular alignment induced by ultrashort laser pulses and its impact on molecular motion. *Israel Journal of Chemistry*, 52(5):414–437, 2012.
- [42] M. Leshko, R. V. Krems, J. M. Doyle, and S. Kais. Manipulation of molecules with electromagnetic fields. *Molecular Physics*, 111(12-13):1648–1682, 2013.
- [43] B. A. McGuire, P. B. Carroll, R. A. Loomis, I. A. Finneran, P. R. Jewell, A. J. Remijan, and G. A. Blake. Discovery of the interstellar chiral molecule propylene oxide (CH₃CHCH₂O). *Science*, 352(6292):1449–1452, 2016.
- [44] M. J. Frisch, G. W. Trucks, H. B. Schlegel, G. E. Scuseria, M. A. Robb, J. R. Cheeseman, G. Scalmani, V. Barone, G. A. Petersson, H. Nakatsuji, X. Li, M. Caricato, A. V. Marenich, J. Bloino, B. G. Janesko, R. Gomperts, B. Mennucci, H. P. Hratchian, J. V. Ortiz, A. F. Izmaylov, J. L. Sonnenberg, D. Williams-Young, F. Ding, F. Lipparini, F. Egidi, J. Goings, B. Peng, A. Petrone, T. Henderson, D. Ranasinghe, V. G. Zakrzewski, J. Gao, N. Rega, G. Zheng, W. Liang, M. Hada, M. Ehara, K. Toyota, R. Fukuda, J. Hasegawa, M. Ishida, T. Nakajima, Y. Honda, O. Kitao, H. Nakai, T. Vreven, K. Throssell, J. A. Montgomery, Jr., J. E. Peralta, F. Ogliaro, M. J. Bearpark, J. J. Heyd, E. N. Brothers, K. N. Kudin, V. N. Staroverov, T. A. Keith, R. Kobayashi, J. Normand, K. Raghavachari, A. P. Rendell, J. C. Burant, S. S. Iyengar, J. Tomasi, M. Cossi, J. M. Millam, M. Klene, C. Adamo, R. Cammi, J. W. Ochterski, R. L. Martin, K. Morokuma, O. Farkas, J. B. Foresman, and D. J. Fox. Gaussian 16, Revision A.03, 2016.
- [45] L.D. Landau and E.M. Lifshitz. *Mechanics*. Butterworth-Heinemann, Oxford, Third edition, 1976.
- [46] D. C. Rapaport. *The Art of Molecular Dynamics Simulation*. Cambridge University Press, 2 edition, 2004.
- [47] L. Romero E. A. Coutias. The quaternions with an application to rigid body dynamics. Techreport, University of New Mexico, Albuquerque, NM 87131, Feb 1999.
- [48] J. B. Kuipers. *Quaternions and Rotation Sequences: A Primer with Applications to Orbits, Aerospace and Virtual Reality*. Princeton University Press, 2002.
- [49] S. M. LaValle. *Planning Algorithms*. Cambridge University Press, New York, NY, USA, 2006.
- [50] M. Spanner and M. Yu. Ivanov. Angular trapping and rotational dissociation of a diatomic molecule in an optical centrifuge. *The Journal of Chemical Physics*, 114(8):3456–3464, 2001.
- [51] M. Spanner, K. M. Davitt, and M. Yu. Ivanov. Stability of angular confinement and rotational acceleration of a diatomic molecule in an optical centrifuge. *The Journal of Chemical Physics*, 115(18):8403–8410, 2001.
- [52] T. Armon and L. Friedland. Capture into resonance and phase-space dynamics in an optical centrifuge. *Phys. Rev. A*, 93:043406, Apr 2016.
- [53] T. Armon and L. Friedland. Quantum versus classical dynamics in the optical centrifuge. *Phys. Rev. A*, 96:033411, Sep 2017.
- [54] V. Milner. Typical parameters of the optical centrifuge. Private communication, 2017.
- [55] A. Steinbacher, H. Hildenbrand, S. Schott, J. Buback, M. Schmid, P. Nuernberger, and T. Brixner. Generating laser-pulse enantiomers. *Opt. Express*, 25(18):21735–21752, Sep 2017.
- [56] E. Gershnel, I. Sh. Averbukh, and Robert J. Gordon. Orientation of molecules via laser-induced antialignment. *Phys. Rev. A*, 73:061401, Jun 2006.
- [57] E. Gershnel, I. Sh. Averbukh, and R. J. Gordon. Enhanced molecular orientation induced by molecular antialignment. *Phys. Rev. A*, 74:053414, Nov 2006.